

## Supplementary Information

# Oleo-Furan and Branched Surfactants Made from Recycled and Renewable Feedstocks

*Darien K. Nguyen<sup>†1,2</sup>, Tejas Goculdas<sup>†1</sup>, Mahdi A. Al Ismail<sup>1</sup>, Caroline Kulp<sup>1</sup>, Sunitha Sadula<sup>3</sup>,  
Dionisios G. Vlachos<sup>\*1,2,3</sup>*

1 – Department of Chemical and Biomolecular Engineering, University of Delaware,  
Newark, Delaware 19716, United States

2 – Center for Plastics Innovation, University of Delaware, Newark, Delaware 19716, United  
States

3 – Delaware Energy Institute, University of Delaware, Newark, Delaware 19716, United  
States

† Contributed equally.

\* Corresponding author: [vlachos@udel.edu](mailto:vlachos@udel.edu)

## Methods Supplementary Information

### Plasma Reactor and Diagnostics

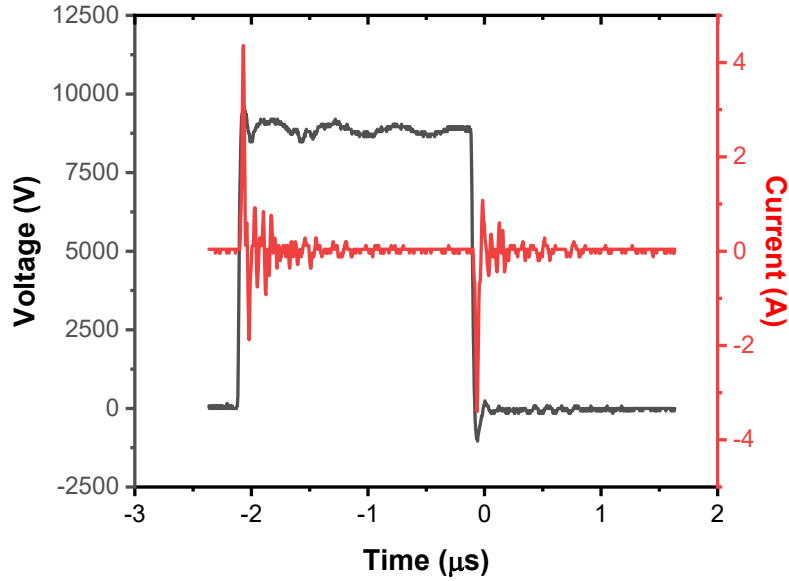


**Figure S1.** Representative current and voltage waveforms in the pulsed DC plasma reactor (calculated power:  $\sim 2.1$  W). Plasma operating conditions: voltage: 9 kV, frequency: 5 kHz, duty cycle: 1%,  $O_2$  feed molar percent: 2%, and temperature: 35 °C.

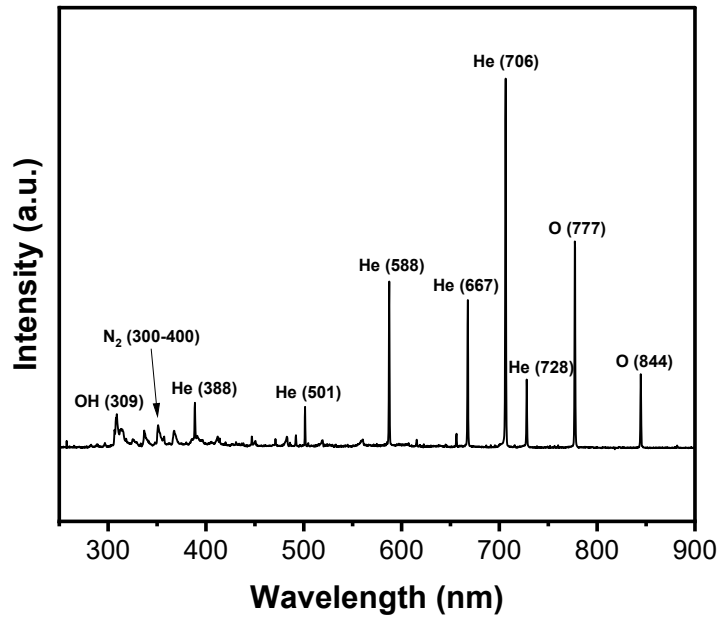


**Figure S2.** Optical emission spectroscopy (OES) spectra of He/ $O_2$  plasma discharge. Plasma operating conditions as in Fig. S1.

## Results and Discussion Supplementary Information

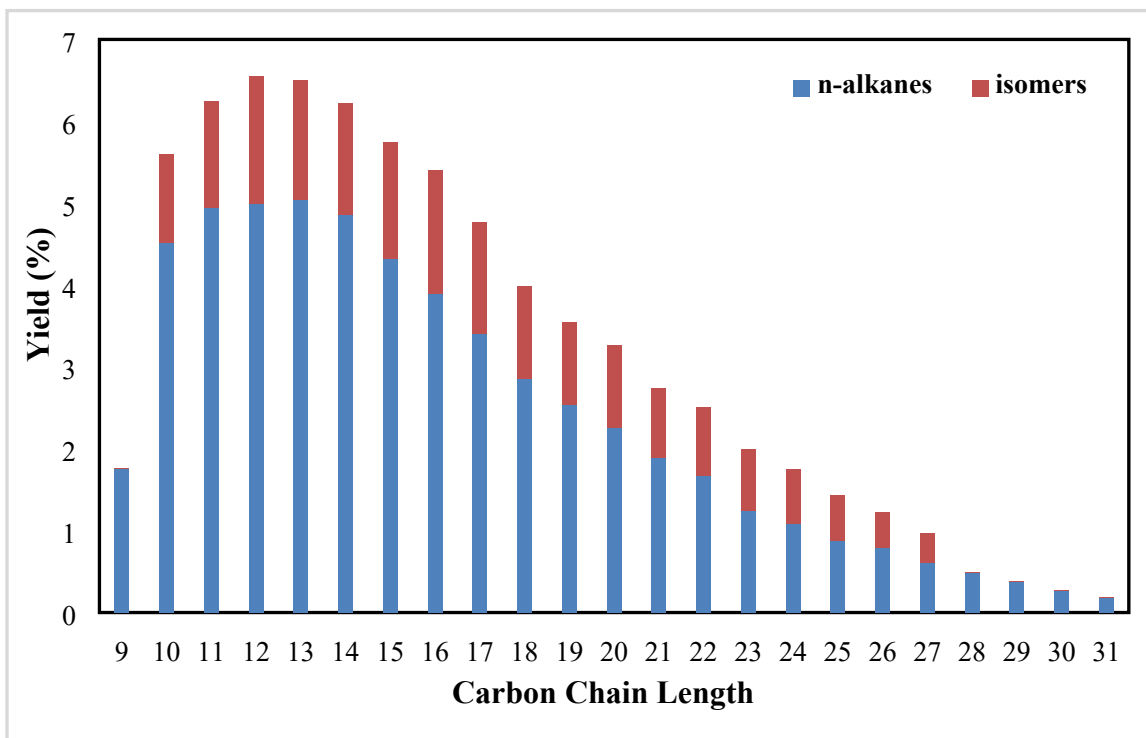


**Figure S3.** Yield percent distribution of n-alkanes and isomers of hydrogenolysis wax. Reaction conditions: catalyst-to-polymer ratio: 0.03, catalyst mass: 0.1 g, treatment time: 4 h, H<sub>2</sub> pressure: 30 bar, stir rate: 400 rpm, and temperature: 250 °C. GC conditions: HP-Innowax column from 30 – 250 °C in dichloromethane.

*C<sub>16</sub> Proof of Concept and Stability Experiments*

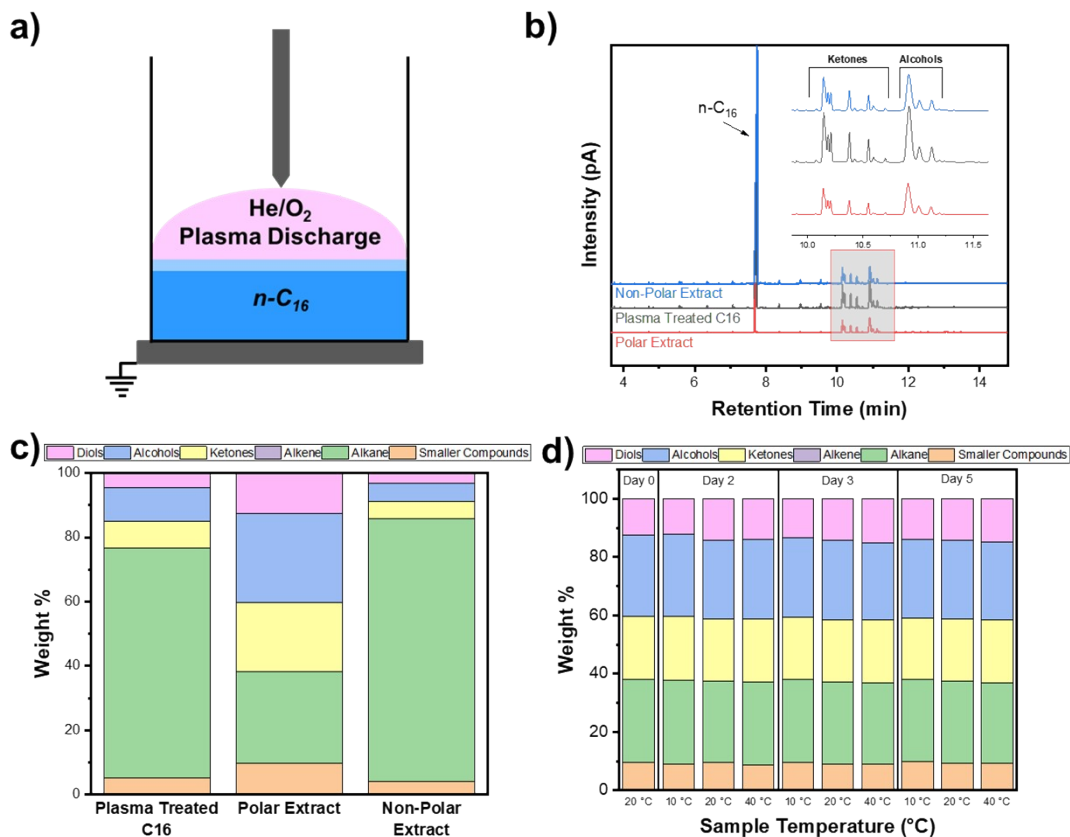


**Figure S4.** (a) Schematic of plasma oxidation of n-C<sub>16</sub> model compound. (b) GC spectra of pre-separated plasma-oxidized C<sub>16</sub>, polar phase extraction, and non-polar phase extraction. (c) Weight percent distribution of n-alkanes and oxygenates in pre-separated plasma-oxidized C<sub>16</sub>, polar phase extraction, and non-polar phase extraction. (d) Weight percent distribution of oxygenates indicating stability over 5 days at different temperatures. Plasma operating conditions as in Fig. S1. GC conditions: HP-Innowax column from 30 – 250 °C in dichloromethane.

## GC Analysis of Post-Plasma-Oxidized Paraffins and Gas Trap

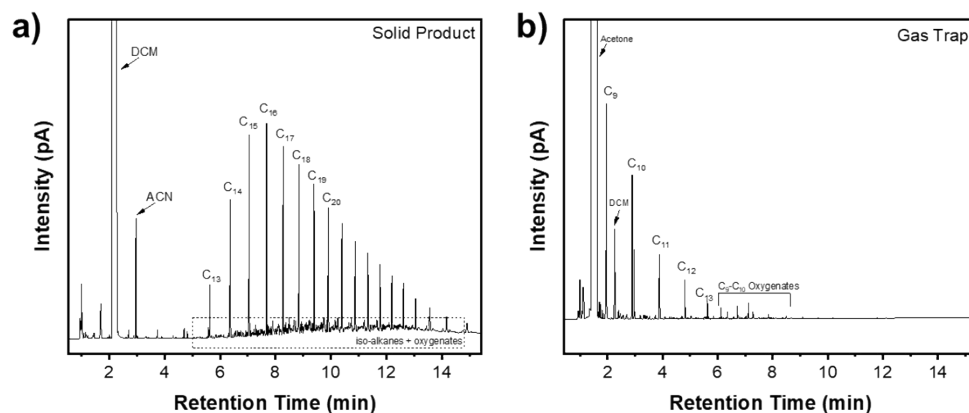


**Figure S5.** GC chromatogram of (a) post-plasma-oxidized paraffins and (b) gas trap collected during plasma-oxidation of hydrogenolysis paraffin. Plasma operating conditions: voltage: 9 kV, frequency: 5 kHz, O<sub>2</sub> feed molar percent: 2%, and temperature: 35 °C. GC conditions: HP-Innowax column from 30 – 250 °C in dichloromethane.

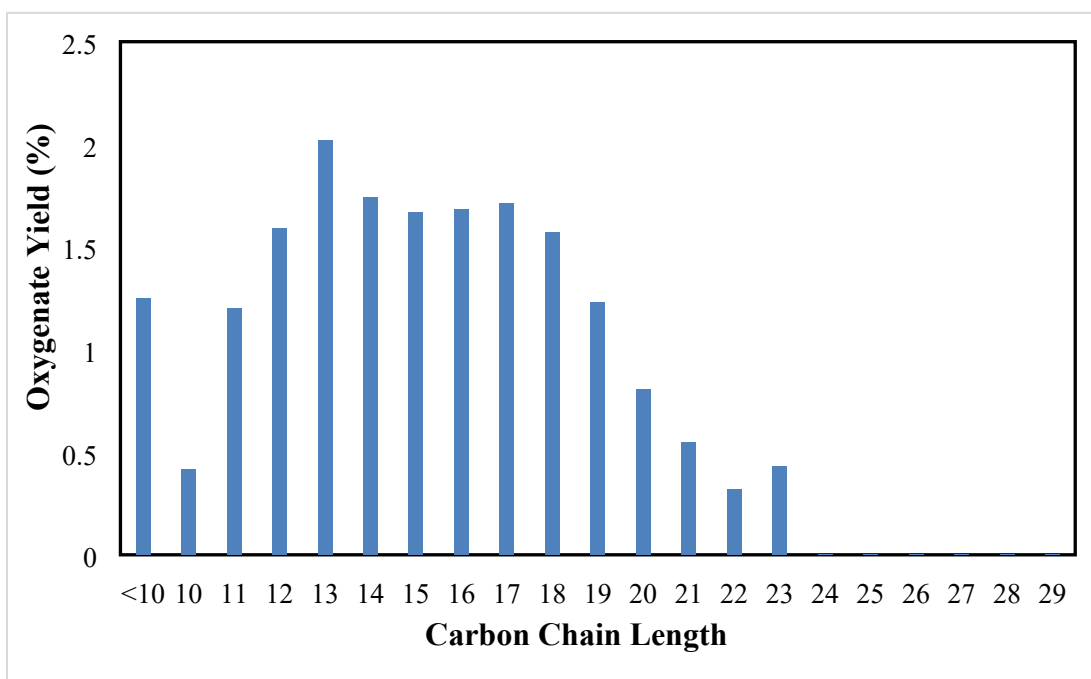


**Figure S6.** Yield percent distribution of oxygenates in plasma-oxidized wax. Plasma operating conditions: voltage: 9 kV, frequency: 5 kHz, O<sub>2</sub> feed molar percent: 2%, and temperature: 30 °C. GC conditions: HP-Innowax column from 30 – 250 °C in dichloromethane.

**Table S1.** Pd/C catalyzed hydrogenation of 6-undecanone and 12-tricosanone. Reaction Conditions: 0.2 g of 5 wt% Pd/C, 3 mmol ketone, 6 h, 150 °C, 30 bar H<sub>2</sub>.

Ketone	Conversion (mol%)	Alcohol Yield (mol%)
6-undecanone	9.4	8.1
12-tricosanone	2.7	N/A

**Table S2.** NaBH<sub>4</sub>-catalyzed reduction of 2-dodecanone and 6-undecanone. Reaction Conditions: 6.7 mmol NaBH<sub>4</sub>, 2.2 mmol ketone, 1 h, 25 °C.

Ketone	Conversion (mol%)	Alcohol Yield (mol%)
2-dodecanone	100	94.6
6-undecanone	100	97.2
2-dodecanone	100	97*

\*Reaction done with an equimolar amount of alcohol and ketone; yield calculated assuming only the ketone reacted; overall yield taking into account the initial moles of alcohol was 197%

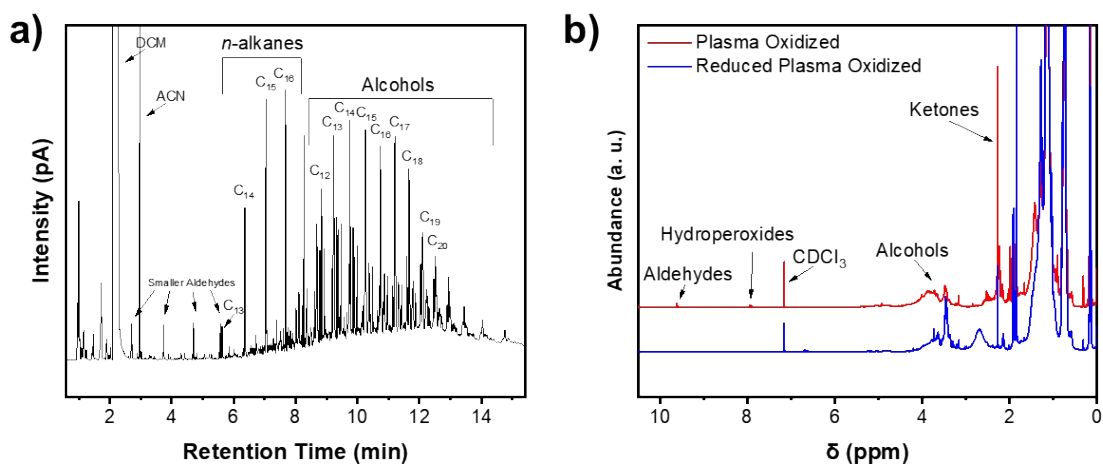


**Figure S7.** (a) GC chromatogram and (b) <sup>1</sup>H-NMR of (a) post-reduction plastic-derived oxygenated paraffins. Plasma operating conditions: voltage: 9 kV, frequency: 5 kHz, O<sub>2</sub> feed molar percent: 2%, and temperature: 35 °C. GC conditions: HP-Innowax column from 30 – 250 °C in dichloromethane. <sup>1</sup>H-NMR conditions: 25 °C in chloroform-d<sub>2</sub>.

### Screening Primary and Secondary Alcohols

Due to the heterogeneity of the oxygen-containing functional groups of the plasma-oxidized stream, we first screened 4 commercially available alcohols of varying chain length and OH group position for esterification. The results are shown in **Figure S8**. The activity is high under these conditions, but product selectivity varied. The 1-dodecanol was selective toward the ester product (94.2 mol%), with a conversion of nearly 100%. 2-dodecanol resulted in significant yields of C<sub>12</sub> olefins (72.7 mol% yield) due to the acid-catalyzed dehydration of the alcohol group. Three isomers of the olefin were observed. Kinetic studies have shown that alcohol substitution is a key determinant of the selectivity of the dehydration reaction<sup>37, 38</sup>. Specifically, the stability of the carbocation (**Scheme S1**) increases with the number of neighboring electron-donating groups, in this case, CH<sub>x</sub> groups. As a result, carbocation and subsequent dehydration are favored in tertiary alcohols, followed by secondary alcohols, and then primary alcohols.

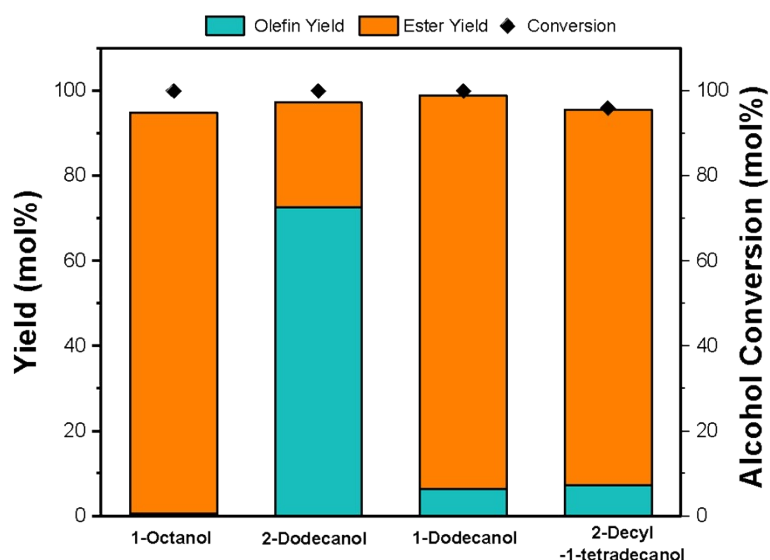


**Figure S8.** Esterification of commercially available alcohols with varying chain length and alcohol position. Reaction conditions: 16 mmol 2-furoic acid, 14 mmol alcohols, 150 °C, 10 mol% H<sub>2</sub>SO<sub>4</sub>, 1 h.

### Impact of Alpha Secondary Alcohol vs. Mid-chain Alcohol and Chain Length

To better understand the role of molecular structure on reactivity, we investigated the effects of hydroxyl group position and alkyl chain length on the esterification and dehydration reactions. Specifically, we compared 2-octanol, 5-nonanol, and 2-dodecanol in time-dependent studies to decouple the effects of substitution from chain length. As shown in **Figure S9**, 5-nonanol exhibited lower overall conversion and a higher selectivity toward olefin than 2-octanol. This difference is attributed to the positioning of the hydroxyl group in the mid-chain region, which may reduce its accessibility for nucleophilic attack on the protonated furoic acid<sup>39</sup>, thereby favoring dehydration over esterification.

We also observed a significant decrease in esterification activity using 2-dodecanol compared to 2-octanol, highlighting the influence of chain length. The longer chain of 2-dodecanol likely introduces steric hindrance. Collectively, these results demonstrate that both hydroxyl group position and chain length play key roles in determining conversion and product selectivity.

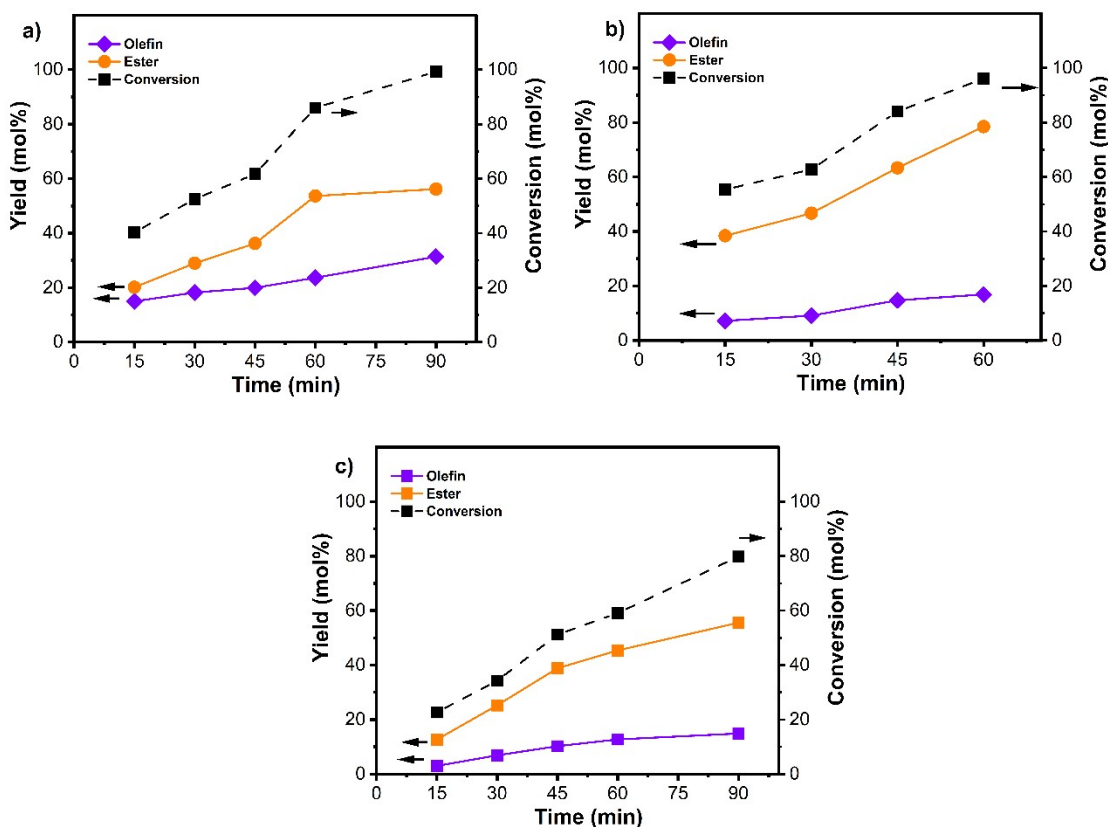
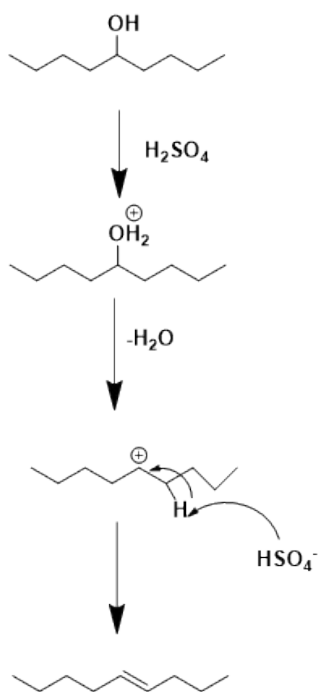
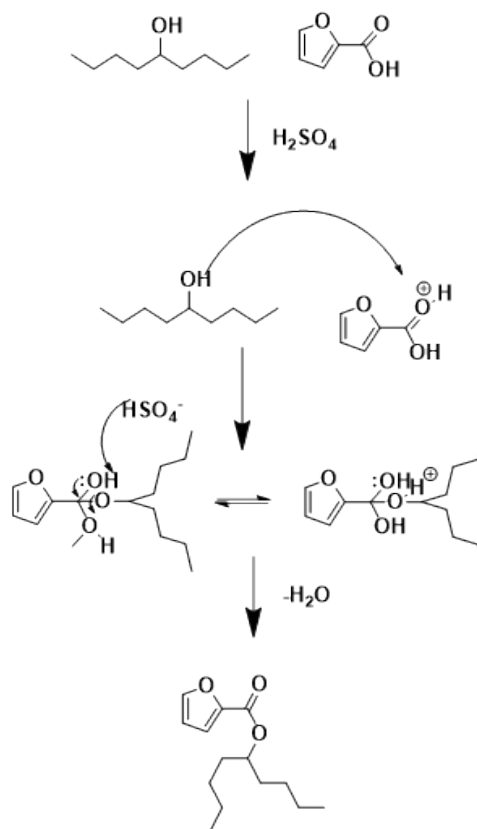


**Figure S9.** Time-dependent studies with varied substitution of the hydroxyl group and alcohol chain length. a) 5-Nonanol, b) 2-Octanol, and c) 2-Dodecanol. Reaction conditions: 1 mol% acid, 12 mmol 2-furoic acid, 11 mmol alcohol, 150 °C.

**a) Acid-Catalyzed Dehydration**



**b) Esterification**



*Scheme S1. Reaction mechanism for a) Acid-catalyzed dehydration and b) Esterification.*

### Optimization of Acid Concentration

POP consists predominantly of secondary alcohols and ketones<sup>25</sup>. To favor esterification over dehydration, we optimize the reaction conditions using 2-dodecanol as a model compound, leveraging existing knowledge. **Scheme S1** depicts the competing reaction pathways. Dehydration to olefins proceeds via a carbocation intermediate formed after protonation of the alcohol. In contrast, Fischer esterification proceeds through protonation of the carboxylic acid, followed by nucleophilic attack by the alcohol<sup>37</sup>. Esterification shows a first-order dependence<sup>40-42</sup> on the acid concentration, whereas dehydration, as demonstrated for xylose, follows a nonlinear but weaker correlation<sup>43</sup>. Overall, dehydration exhibits a higher acid concentration dependence. This was corroborated by control experiments using 2-dodecanol or 2-octanol without an acid, where esterification occurred but no olefin formed (**Table S3**). With this information, we tuned the selectivity by varying the catalyst ( $\text{H}_2\text{SO}_4$ ) loading. The results (**Figure S10**) show a gradual increase in ester selectivity as the acid loading decreased, reaching a maximum of 76.2% at 86.3% conversion at 1 mol%  $\text{H}_2\text{SO}_4$ . As described in the methods, water formed during the reaction was vented through the syringe every 15 min.

**Table S3.** Uncatalyzed esterification reactions of 2-octanol and 2-dodecanol. Reaction conditions: 12 mmol 2-furoic acid, 11 mmol 2-dodecanol, 2 h, 150 °C.

Alcohol	Conversion (mol%)	Olefin Yield (mol%)	Ester Yield (mol%)
2-Octanol	18.5	0	14.2
2-Dodecanol	10.1	0	7.3

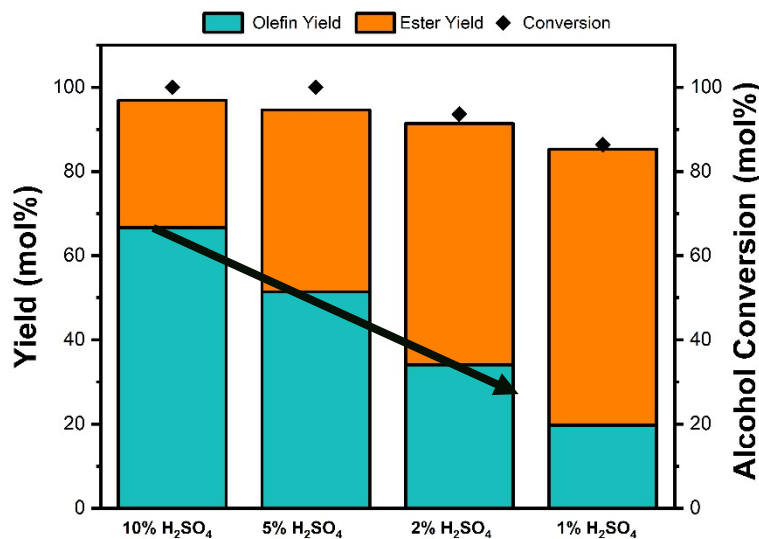


**Figure S10.** Effect of catalyst loading on esterification of 2-dodecanol with 2-furoic acid. Reaction conditions: 12 mmol 2-furoic acid, 11 mmol alcohol, 2 h, 150 °C.

To suppress olefin formation, we screened Lewis acid catalysts, such as zinc oxide, chloride, and acetate, for esterification (**Figure S11**). Unfortunately, this resulted in low alcohol conversion over ZnO (30%), and another ester byproduct and alkyl halide, respectively, over Zn(Ac)<sub>2</sub> and ZnCl<sub>2</sub>. Therefore, we used sulfuric acid as the catalyst.

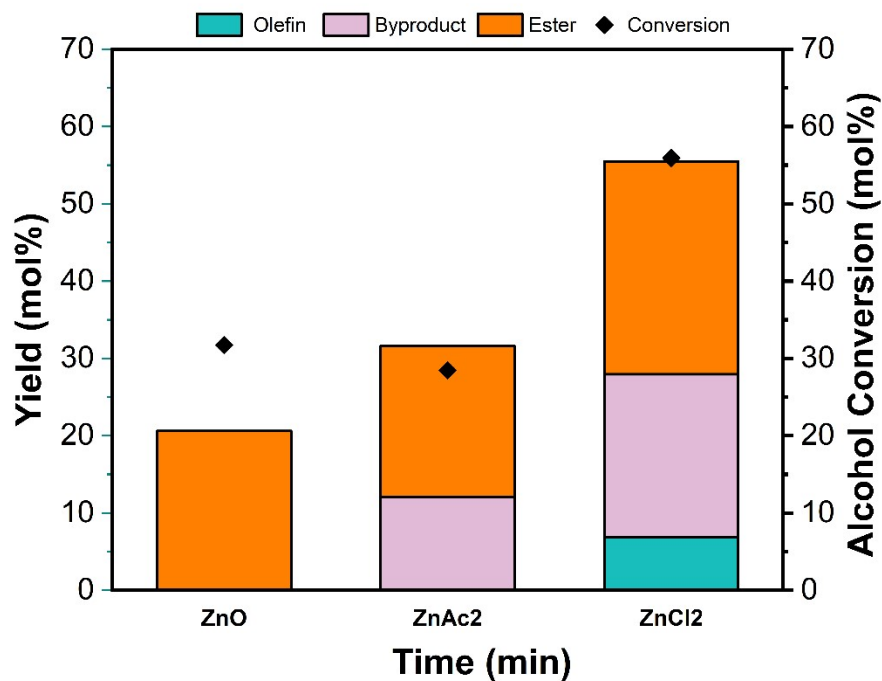


**Figure S11.** Performance of zinc salts for the esterification of 2-octanol with 2-furoic acid. Reaction conditions: 1 mol% catalyst, 12 mmol 2-furoic acid, 11 mmol alcohol, 150 °C.

Based on the trends observed with the model compounds, oxygenates derived from plastics waste are likely to generate appreciable amounts of mid-chain olefins. We explored a strategy to separate the desired furoic esters from olefins via solvent extraction. Due to the hydrophobic nature of the long alkyl chains in both products, aqueous extraction methods proved ineffective. As a result, we screened two miscible organic biphasic systems—methanol/heptane and acetonitrile/heptane—to partition olefins and esters. The crude reaction mixture obtained from the 5 mol% H<sub>2</sub>SO<sub>4</sub> esterification of 2-dodecanol was used as representative for this study.

As summarized in **Table S4**, the acetonitrile/heptane system was more effective than methanol/heptane, achieving nearly complete removal of olefins after a single wash. After two washes, the polar phase contained 98% of the furoic ester and 2% olefin. However, approximately 42% of the ester partitioned into the non-polar phase during the first extraction. This could be mitigated by additional recovery cycles on the non-polar layer to improve overall ester recovery.

**Table S4.** Results from the solvent extraction of 2-furoic esters from the crude reaction mixture in the polar phase.

Solvent System	Polar Layer	Initial Composition	First Wash	Second Wash
MeOH/Heptane	MeOH Layer	43% Ester, 57% Olefin	61% Ester, 39% Olefin	93% Ester, 7% Olefin
	Heptane Layer	N/A	23% Ester, 77% Olefin	30% Ester, 70% Olefin
ACN/Heptane	ACN Layer	43% Ester, 57% Olefin	92% Ester, 8% Olefin	98% Ester, 2% Olefin
	Heptane Layer	N/A	16% Ester, 84% Olefin	80% Ester, 20% Olefin

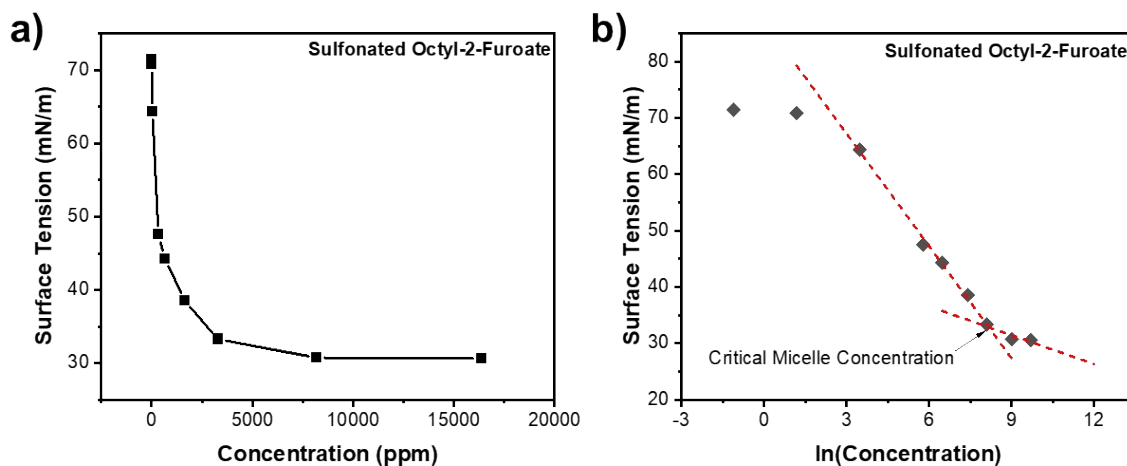


**Figure S12.** (a) Surface tension vs. concentration plot of sulfonated octyl 2-furoate (O2F). (b) Surface tension vs. ln(concentration) plot of O2F with calculated CMC from the intersection of the sloped lines.

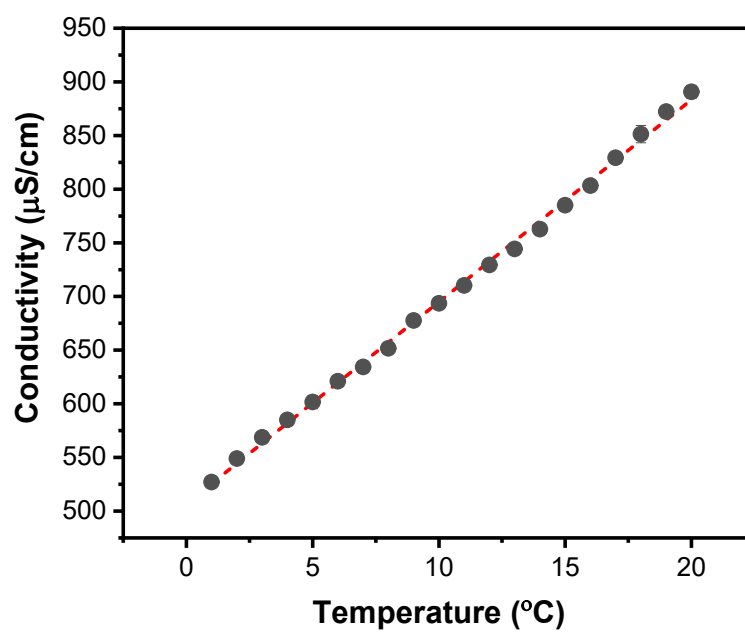


*Figure S13. (a) Conductivity values at various temperatures of octyl 2-furoate (4092 ppm).*

**Table S5.** Comparison of Krafft temperature and CMC of PDOFBS to commercial and various OFS surfactants from previous works.

Surfactant	CMC (ppm)	Krafft Temperature (°C)	Source
Sodium Lauryl Sulfate (SLS)	2010	15.0 ± 1.2	Commercial
Methyl Ester Sulfonate (MES)	130	<0	Commercial
Linear Alkylbenzene Sulfonate (LAS)	460	20.0 ± 2.5	Commercial
Sodium Lauryl Ether Sulfate (SLES)	380	<0	Commercial
Oleo-Furan Sulfonates - 12-1/O	11520	<0	Park et al.
Oleo-Furan Sulfonates - 14-1/O	3127	<0	Park et al.
Oleo-Furan Sulfonates - 18-1/O	1156	<0	Park et al.
Oleo-Furan Sulfonates - Cocinic (8-18)-1/O	4890	<0	Park et al.
Oleo-Furan Sulfonates - 7	2669	<0	Park et al.
Oleo-Furan Sulfonates - 12	720	30	Park et al.
Oleo-Furan Sulfonates - 14	267	41.5	Park et al.
Oleo-Furan Sulfonates - 18	316	>50	Park et al.
Oleo-Furan Sulfonates - Cocinic (8-18)	512	18.5	Park et al.
40:60 mol% OFS-12-2/C <sub>2</sub> H <sub>5</sub> :OFS-12	510	25.7	Park et al.
85:15 mol% OFS-12-1/O:OFS-12	2445	< 0	Park et al.
Sulfonated Alkyl Furoates - 8	1332	< 0	Al Ghatta et al.
Sulfonated Alkyl Furoates - 12	521	22-25	Al Ghatta et al.
Sulfonated Alkyl Furoates - 16	60	48	Al Ghatta et al.
Plastic-Derived Oleo-furan and branched sulfonates	591	< 0	This work

**Table S6.** Computational ecotoxicity simulations on C<sub>14</sub>furoic ester and C<sub>14</sub> alkylbenzene.

<b>Property</b>	<b>C<sub>14</sub> Furoic ester</b>	<b>C<sub>14</sub> Alkylbenzene</b>	<b>Comment</b>
Log (K <sub>ow</sub> )	6.84	7.79	Log (K <sub>ow</sub> ) is a measure of the partition coefficient between aqueous and organic phases, lower the better
Biodegradation Potential (Linear Model Prediction)	0.89	0.9147	
Biodegradation Potential (Non-Linear Model Prediction)	0.9914	0.9715	
Bioconcentration Factor (Log <sub>10</sub> )	1.15	2.56	Time taken for the compound to reach 50% of its initial concentration in an aqueous stream
Fathead Minnow Toxicity (mg/L)	1.03	0.27	LC50 towards the fathead minnow, higher the better

**Table S7.** Overall catalytic efficiency of each process step for generating surfactants from plastic waste.

<b>Process Step</b>	<b>Catalytic Efficiency (%)</b>
1) Plastic Hydrogenolysis	73
2) Plasma Oxidation	54
3) Sodium Borohydride Reduction	95
4) Furoic Acid Esterification	96
5) Sulfonation	87
Overall Efficiency	31

*Table S8. Preliminary TEA analysis of the entire process scheme.*

<b>Process Step</b>	<b>Reagent</b>	<b>Cost (\$/kmol surfactant)</b>	<b>Percent of Cost</b>
Plastic Hydrogenolysis	Hydrogen	16	1.5%
Plasma Oxidation	Plasma (electricity)	607.8	56.5%
Sodium Borohydride Reduction	Sodium Borohydride (NaBH <sub>4</sub> )	30.4	2.8%
Furoic Acid Esterification	2-furoic acid	178.8	16.6%
	Sulfuric Acid (H <sub>2</sub> SO <sub>4</sub> )	0.6	0.05%
Sulfonation	Chlorosulfonic Acid (ClSO <sub>3</sub> H)	58	5.4%
	Sodium Bicarbonate (NaHCO <sub>3</sub> )	13.9	1.3%

This preliminary TEA was calculated based on 5 assumptions:

1. Slight excesses of reactants were used as opposed to laboratory conditions, which were larger excesses due to the constraints of how much material we were working with.
2. Ru/TiO<sub>2</sub> catalyst was reusable in plastic hydrogenolysis.
3. Capital costs and operating costs of separations were not included.
4. Assumed that the total cost of reactants is ~80% of the total production cost.
5. Assume the final mixture is an average of 25% furoates and 75% branched sulfonates.